



Title of proposed experiment:

Measurement of the Astrophysical Rate of the  $^{21}\text{Na}(p,\gamma)^{22}\text{Mg}$  Reaction

Name of group: SODIUM

Spokesperson for group: J.M. D'Auria / N.P.T. Bateman

E-Mail address: dauria@sfu.ca Fax number: 604-222-1074

Members of the group (name, institution, status, per cent of time devoted to experiment)

<u>Name</u>	<u>Institution</u>	<u>Status</u>	<u>Time</u>
J.M. D'Auria	Simon Fraser University	Professor	NA
N.P.T. Bateman	Simon Fraser University	Research Associate	NA
R.N. Boyd	Ohio State University	Professor	NA
L. Buchmann	TRIUMF	Research Scientist III	NA
U. Giesen	Simon Fraser University/TRIUMF	Research Associate	NA
U. Greife	Ruhr-Universität Bochum	Research Scientist	NA
R. Helmer	TRIUMF	Research Scientist	NA
D. Hunter	Simon Fraser University	Research Associate	NA
A. Hussein	University of Northern British Columbia	Professor	NA
D. Hutcheon	TRIUMF	Senior Research Scientist	NA
K.P. Jackson	TRIUMF	Senior Research Scientist	NA
J.D. King	University of Toronto	Professor	NA
R. Korteling	Simon Fraser University	Professor	NA
S. Kubono	Center for Nuclear Study, U. of Tokyo	Professor	NA
T. Motobayashi	Rikkyo University	Professor	NA
A. Olin	TRIUMF	Senior Research Scientist	NA
P.D. Parker	Yale University	Professor	NA
C. Rolfs	Ruhr-Universität Bochum	Professor	NA
J. Rogers	TRIUMF	Senior Research Scientist	NA
G. Roy	University of Alberta	Professor Emeritus	NA
A. Shotton	University of Edinburgh	Professor	NA
F. Strieder	Ruhr-Universität Bochum	Grad. Student	NA
H.-P. Trautvetter	Ruhr-Universität Bochum	Senior Research Scientist	NA
M. Wiescher	University of Notre Dame	Professor	NA



Start of preparations: January 2000	Beam time requested:		
Date ready: July 2000	12-hr shifts	Beam line/channel	Polarized primary beam?
Completion date: 2002	~50 ( $^{21}\text{Na}$ )	2A/ISAC	No
	~50 (stable)	na/ISAC	na

The  $^{21}\text{Na}(p,\gamma)^{22}\text{Mg}$  reaction plays a key role in the astrophysical production of the radioactive nuclide  $^{22}\text{Na}$ . This nuclide is important as a target for current and future generations of gamma ray telescopes, and because its daughter,  $^{22}\text{Ne}$ , has been found in pre-solar grains in meteorites. The production of  $^{22}\text{Na}$  is therefore a diagnostic of models of explosive nucleosynthesis in the present day Galaxy, and in the Galaxy at the time of formation of the solar system.

In astrophysical environments the  $^{21}\text{Na}(p,\gamma)^{22}\text{Mg}$  reaction is believed to be dominated by a single resonance at 212 keV in the centre of mass frame[1]. Complete spectroscopic information on the states through which this and higher lying resonances proceed is not known, so resonance strengths have to be predicted by using spectroscopic information from the mirror nucleus  $^{22}\text{Ne}$ . As a result the  $^{21}\text{Na}(p,\gamma)^{22}\text{Mg}$  reaction rate is not well known. We propose to measure the resonance strengths of all three of the resonances that lie in the astrophysically important energy regime. All of these resonances are almost certainly very narrow ( $\ll 1$  keV), and so the narrow resonance formalism can be used to calculate the reaction rate at all relevant temperatures once we have measured the resonance reaction rates. Such rate information would be extremely useful in constraining models of explosive nucleosynthesis.

We propose to measure these three reaction rates using the DRAGON facility in the high energy area of the ISAC experimental hall. The full facility will consist of a differentially pumped gas target, a recoil mass separator, and an array of gamma detectors, all of which will be optimized to measure capture reactions. As noted above, we do not have adequate spectroscopic data to accurately predict the resonance strengths that we will measure, but we expect low yields. Therefore measurement of this reaction rate requires the use of a recoil mass separator with excellent beam rejection. As will be discussed the DRAGON should meet our needs. The necessary rejection will be achieved by detecting the recoiling  $^{22}\text{Mg}$  nuclei at the final focus of the recoil separator and measured the capture  $\gamma$  rays in coincidence. The gamma array will also provide more detailed information on the resonances.

With a beam current of  $10^{10}$  atoms/s we expect data rates of 15 - 100 real events per hour. The measured rates may be very different from this, because the resonance strengths of these resonances are not well known. However, a 20% measurement of each of the resonance strengths would be more than adequate for astrophysical purposes, and in principle such a measurement could be made in a single 12 hour shift. Beams of  $^{21}\text{Na}$  should be relatively easy to produce with the surface ionization source, which is scheduled to be the first source available at ISAC. The ready availability of the beam, and the relatively high counting rates in this experiment mean that the  $^{21}\text{Na}(p,\gamma)^{22}\text{Mg}$  reaction would be a good choice for the first experiment to be performed with high energy beams at ISAC. Finally, we note that we will also require considerable stable beam time on the linac to understand our efficiencies.

## Experimental area

ISAC high energy hall (DRAGON)

## Primary beam and target (energy, energy spread, intensity, pulse characteristics, emittance)

proton (10  $\mu$ A, 500 MeV, CW)

Unpolarized

## Secondary channel ISAC

## Secondary beam (particle type, momentum range, momentum bite, solid angle, spot size, emittance, intensity, beam purity, target, special characteristics)

ISAC ion source:  $^{21}\text{Na}$ , 200-1500 keV/u, bunched beam ( $\Delta t \simeq 1$  ns,  $\Delta E/E \simeq 0.2\%$ )off-line ion source:  $^{21}\text{Ne}$ ,  $^{22}\text{Ne}$ ,  $^{23}\text{Na}$ ,  $^{24}\text{Mg}$ , .15-1.5 MeV/u

## TRIUMF SUPPORT:

- ISAC
- ion source development (on-line and off-line)
- technical and engineering support for design, construction and operation of DRAGON facility
- pool electronics
- data acquisition support

## NON-TRIUMF SUPPORT

NSERC support will be sought for experimental facilities and project support

- DRAGON facility
  - windowless gas target
  - gamma array
  - electromagnetic recoil separator
  - carbon foil/micro-channel plate detectors and parallel grid avalanche counter/ion chamber gas detector for use at the final focus
  - detector electronics
- project support for students and RAs, travel etc.

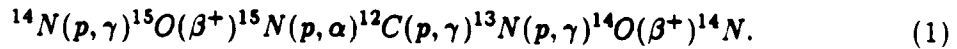
The safety concerns for this experiment are largely the same as those of the ISAC facility as a whole. These are discussed in the ISAC safety report. Safety concerns specific to this experiment are:

1. Radiation fields generated using up to  $10^{11}$  atoms/s of  $^{21}\text{Na}$ . This corresponds to 100 GBq if stopped in one location.  $^{21}\text{Na}$  is a  $\beta^+$  emitter with a branching ratio of 100%, and an end point of 2.5 MeV. Up to 70% of this activity could be deposited at the bending magnet in the medium energy beam transport, the remainder would be deposited in the electromagnetic separator of the DRAGON. A rough estimate of the dose due to 70% of this beam is about 100 mSv/h at a distance of 1 m. However, this activity should be very well localized, and should be relatively simple to shield. At the 1% level (i.e.,  $\leq 1$  GBq) activity could be deposited anywhere along the beam line and accelerator. The half-life of  $^{21}\text{Na}$  is only 22 s, so there will only be significant fields present while the beam is on, and for a few minutes thereafter. Once the beam has been tuned it will be easy to locate and shield the hot spots. While the beam is on target, personnel will have to be excluded from the area near the accelerator and recoil separator. This will have to be done through interlocked gates.
2. Hazards of using hydrogen gas as a target.

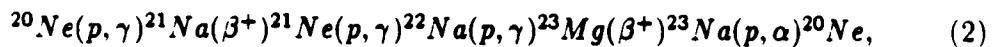
## 1 Scientific Justification

### 1.1 Nucleosynthesis in Novae

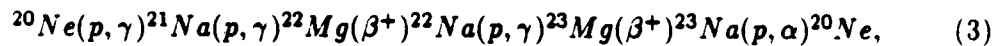
Novae occur on the surfaces of white dwarf stars that accrete matter from a companion star. The accreted material gains a large amount of energy as it falls into the gravitational field of the white dwarf, and this energy heats the surface layer. When the temperature is high enough to ignite thermonuclear reactions an explosion ensues. The material transferred from the companion star has solar composition, so the explosion takes place in a hydrogen-rich environment where  $(p,\gamma)$  reactions will predominate. Because most white dwarfs are composed of carbon and oxygen, and because carbon and oxygen are the dominant heavy elements in material of solar composition, the dominant hydrogen-burning mechanism in novae is the well understood HotCNO cycle,



However, over the past decade or so, a separate class of novae has been observed. The ejecta of these novae are strongly enriched in neon, sodium, magnesium and aluminum, and they are known as Ne novae. They are understood to be novae in which the underlying white dwarf is composed of oxygen and neon. If the material from the white dwarf mixes with the hydrogen-rich material that is accreted then the ejecta abundances are readily explained. In this scenario the hydrogen burning during the nova outburst could be dominated by the NeNa cycle (see figure 1),



and



which is much less well understood than the HotCNO cycle. (Note that the time scales for nova explosions are much too short for  ${}^{22}\text{Na}$  to decay.) Because the warm NeNa cycle (equation 2) includes the  $\beta$  decay of  ${}^{21}\text{Na}$ , the rate of energy generation in this cycle is limited by this decay, which has a 22 second half-life. By bypassing this decay, the hot NeNa cycle (equation 3) can increase the energy generation during the explosion. To understand the energy generated during a nova outburst, and thus to understand the hydrodynamics, it is very important to understand the temperatures and densities at which the transition from the warm NeNa cycle (equation 2) to the hot NeNa cycle (equation 3) takes place. The rate of the  ${}^{21}\text{Na}(p,\gamma){}^{22}\text{Mg}$  reaction determines when this transition takes place, so it plays a key role in our understanding of this type of nova.

The  ${}^{22}\text{Mg}$  beta decay will probably not be bypassed in most explosions because the  ${}^{22}\text{Mg}(p,\gamma){}^{23}\text{Al}$  reaction has a Q-value of only 125 keV. The low Q-value means that  ${}^{23}\text{Al}$  is readily photo-disintegrated and cannot be built up in large abundances. Consequently, at very high temperatures the  ${}^{22}\text{Mg}$  beta decay can become a bottleneck in the hot NeNa cycle, and  ${}^{22}\text{Mg}$  can be present in large abundances. At the end of the explosion all of the  ${}^{22}\text{Mg}$  will decay to  ${}^{22}\text{Na}$ . Therefore, the rate of the  ${}^{21}\text{Na}(p,\gamma){}^{22}\text{Mg}$  reaction also affects how much of the astrophysically interesting nucleus,  ${}^{22}\text{Na}$  is produced by explosive hydrogen burning.

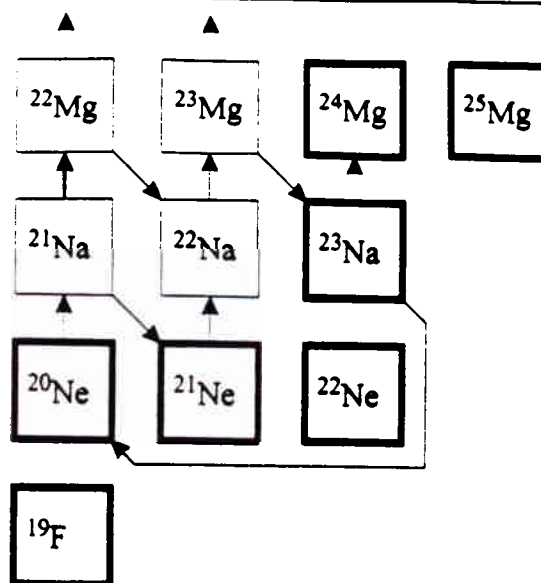


Fig. 1 Neon Sodium Cycles. Stable nuclides are shown with dark outlines, and the solid lines represent reactions and decays in the two branches of the NeNa cycle. Dashed lines represent reactions that lead to break-out from the NeNa cycle. The cycle that does not pass through  $^{22}\text{Mg}$  is the 'warm' NeNa cycle, the one that does is the 'hot' NeNa cycle.

## 1.2 Meteoritic $^{22}\text{Ne}$

The radioactive nucleus  $^{22}\text{Na}$  is of interest because it decays with the emission of a 1.27 MeV gamma ray, and because its daughter,  $^{22}\text{Ne}$ , has been found in meteorites.

It has now been nearly thirty years since Ne-E was first found in carbonaceous meteorites[2]. This gaseous component consists of neon which is enriched in  $^{22}\text{Ne}$  by factors of as much as 1000. In other words, it is nearly pure  $^{22}\text{Ne}$ . Ne-E in meteorites is carried by small grains of silicon carbide and graphite; because of their anomalous isotopic composition these grains must predate the solar system. They are understood to have formed shortly after individual nucleosynthesis events. One possible site for the formation of these grains is novae, but other sites are possible, including AGB stars, Wolf-Rayet stars, and supernovae (or indeed, some combination of these). Because neon is a noble gas, if at the time of grain formation there was still some  $^{22}\text{Na}$  in the ashes of such an event it would have naturally been incorporated into these grains much more efficiently than any neon. If, in addition, the grains into which the  $^{22}\text{Na}$  had been incorporated were large enough to trap the  $^{22}\text{Ne}$  daughter atoms, these grains would be expected to be strongly enriched in  $^{22}\text{Ne}$ . This is the standard scenario for the origin of Ne-E. However, the half-life of  $^{22}\text{Na}$  is only 2.6 years, and this short half-life means that there are difficulties with this simple picture. For instance, the details of the formation of relatively large grains on such short time scales, and of the effect of the energy released in the beta decay on the survival of these grains must be considered[3].

The isolation of individual grains of graphite and silicon carbide that carry the Ne-E has led to much work on correlating Ne-E with other isotopic anomalies in individual grains (for example, see [4]). By comparing the anomalies in the grains with the predicted isotopic



yields of different nucleosynthesis sites it may be possible to determine the astrophysical sites at which individual grains were formed (for example [5]). If such a stellar source identification could be made with certainty, isotopic abundances measured in the lab could be used to test stellar models. Comparisons between nucleosynthesis in the present day Galaxy and in the Galaxy of 4.5 billion years ago could be made, and a host of other opportunities to expand our understanding of nucleosynthesis could open up. But a strong association of grains with their stellar sources cannot be made until the problems of the time scale for grain formation in various astrophysical sites, and the related problem of the total production of  $^{22}\text{Na}$  in various astrophysical sites are resolved. The total yield of  $^{22}\text{Na}$  from each possible stellar source is largely determined by the conditions under which the Ne/Na cycle operates and, as noted above, our understanding of the operation of this cycle is limited by our lack of knowledge of the  $^{21}\text{Na}(p,\gamma)^{22}\text{Mg}$  reaction rate.

### 1.3 Gamma Ray Astronomy

Another important role that  $^{22}\text{Na}$  can play in astrophysics is as a target for gamma ray astronomy. The  $\beta$  decay of  $^{22}\text{Na}$  is accompanied by the emission of a 1.27 MeV  $\gamma$ -ray. The 2.6 year half-life of  $^{22}\text{Na}$  makes it a very useful probe of recent nova activity; it lives long enough to last until the nova ejectum becomes transparent to gamma rays, but is sufficiently short lived that detection of this line probes only very recent activity. Recent gamma ray astronomy has provided two different ways to test nova models. The flux of 1.27 MeV gamma rays predicted by theoretical models (e.g., [6]) should allow the COMPTEL gamma ray telescope on NASA's Gamma Ray Observatory (GRO) to observe this line from individual Ne novae within 1 kpc of the sun. Such an observation would allow a detailed (and temperature independent) determination of the mass of  $^{22}\text{Na}$  ejected from individual novae, which would provide very useful constraints on nova models. The same theoretical models also predict that diffuse emission of this line from the Galactic centre should be observable by the GRO. The Galactic nova rate is rather uncertain, but is predicted to be around  $100 \text{ yr}^{-1}$  [7]. Much of this uncertainty arises because the Galaxy is dusty and optically thick, so that we can only observe novae that are close to the sun. In general around five novae are seen each year. Most of the novae in the Galaxy should occur near the Galactic centre where the density of stars is the highest. Although  $^{22}\text{Na}$  gamma rays from individual novae at such a large distance are not observable, the accumulation of  $^{22}\text{Na}$  from a large number of novae should lead to an observable flux. Observation of this flux would then constrain models of novae and the Galactic nova rate, and could test whether novae at the Galactic centre (which can only be 'seen' by looking at gamma rays) are similar to nearby novae.

Although the GRO was expected to observe the 1.27 MeV line from  $^{22}\text{Na}$  it has not. Iyudin et al. [8] set upper limits of the  $^{22}\text{Na}$  flux from several individual Ne novae. In particular their upper limit for nova Her 1991 is at least 3 times smaller than the model prediction, and their limit for nova Cyg 1992 is 6 to 30 times below the prediction. In addition the upper limit on the diffuse emission of  $^{22}\text{Na}$  from the Galactic centre is several times smaller than expected [9]. These results strongly suggest that current nova models have serious deficiencies. Although there are several possibilities for the shortcomings of the theoretical models, inaccurate reaction rates cannot be ruled out. As we will show, the reaction rate for  $^{21}\text{Na}(p,\gamma)^{22}\text{Mg}$  is far from certain. Coc et al. [10] suggest that an increased  $^{21}\text{Na}(p,\gamma)^{22}\text{Mg}$  reaction rate would reduce the yield of  $^{22}\text{Na}$ . Effectively a higher



$^{21}\text{Na}(p,\gamma)^{22}\text{Mg}$  rate bypasses the  $^{21}\text{Na}$  half-life of 22 seconds (see figure 1) and leads to  $^{22}\text{Na}$  production at higher temperatures and densities where it is more readily destroyed. In any event, the implications of these upper limits on the  $^{22}\text{Na}$  results cannot be resolved until reasonably accurate reaction rates are available. The experiment that we propose to conduct will provide such a rate for the  $^{21}\text{Na}(p,\gamma)^{22}\text{Mg}$  reaction.

#### 1.4 Astrophysical Reaction Rate for Reactions Dominated by Narrow, Isolated Resonances

Like many capture reactions, the  $^{21}\text{Na}(p,\gamma)^{22}\text{Mg}$  reaction is dominated by narrow isolated resonances. A calculation by Wiescher et al.[11] has shown that the direct capture component can be neglected. Ultimately, we are not interested in making a very high accuracy determination of the  $^{21}\text{Na}(p,\gamma)^{22}\text{Mg}$  reaction rate; we would hope to measure the resonant reaction rates to about 20%. At this level of accuracy we can almost certainly ignore direct capture. The formalism to determine the rate (as a function of temperature and density of a reaction which is dominated by narrow isolated resonances is well developed (e.g., [12]). We summarize it here to demonstrate how our measurements will allow an accurate determination of the astrophysical reaction rate.

In any stellar environment in thermal equilibrium the rate of any reaction is given by,

$$r(\rho, T, \dots) = N_p N_{21} \int_0^{\infty} \phi(v) v \sigma(v) dv, \quad (4)$$

where  $\rho$  is the density,  $T$  is the temperature,  $\phi(v)$  is the Maxwell-Boltzmann distribution,  $\sigma$  is the cross section,  $v$  is the relative velocity of the two nuclei, and  $N_p$  and  $N_{21}$  are the densities of protons and  $^{21}\text{Na}$  ions respectively. Note that we use these nuclides as examples; the formalism that follows generalizes to all reactions through narrow, isolated resonances. Equation 4 is usually simplified to

$$r(\rho, T, \dots) = N_p N_{21} \langle \sigma v \rangle (T), \quad (5)$$

where  $\langle \sigma v \rangle (T)$  is the expected value of the integral in equation 4 as a function of temperature. This is the number we need to find experimentally.

If the reaction rate is dominated by isolated resonance contributions (so that there is no interference between resonances) the total cross section for any resonance is

$$\sigma_i(E) = \pi \lambda^2 \frac{2J_i + 1}{(2J_p + 1)(2J_{21} + 1)} \frac{\Gamma_p^i \Gamma_\gamma^i}{(E - E_i)^2 + (\Gamma_{TOT}^i/2)^2} \quad (6)$$

$$= \pi \lambda^2 (\omega\gamma)_i \frac{\Gamma_{TOT}^i}{(E - E_i)^2 + (\Gamma_{TOT}^i/2)^2}, \quad (7)$$

where  $E$  is the energy in the cm,  $\lambda$  is the reduced de Broglie wavelength (in the cm),  $J_i$ ,  $J_p$  and  $J_{21}$  are the spins of the resonance, the proton, and the  $^{21}\text{Na}$  ground state respectively,  $\Gamma_{TOT}^i$ ,  $\Gamma_p^i$  and  $\Gamma_\gamma^i$  are the total width, proton partial width and gamma partial width of the resonance, and  $E_i$  is the resonance energy.  $(\omega\gamma)_i$  is the resonance strength for each resonance that can play a role at astrophysical energies.

For a narrow resonance the Maxwell-Boltzmann distribution does not change significantly over the resonance (for  $^{21}\text{Na}(p,\gamma)^{22}\text{Mg}$  the broadest resonance of astrophysical

interest is estimated[1] to have a width of 5 eV at a resonance energy of 464 keV) and we can assume that it is constant. Substituting the explicit form of the Maxwell-Boltzmann distribution into equation 4 we get

$$\begin{aligned} \langle \sigma v \rangle (T) &= \sum_i \sqrt{\frac{8}{\pi \mu}} \frac{1}{(kT)^{3/2}} E_i \exp\left(-\frac{E_i}{kT}\right) \\ &\quad \times \int_0^\infty \pi \lambda^2(\omega\gamma)_i \frac{\Gamma_{TOT}^i}{(E - E_i)^2 + (\Gamma_{TOT}^i/2)^2} dE \end{aligned} \quad (8)$$

$$= \left(\frac{2\pi}{\mu kT}\right)^{3/2} \hbar^2 \sum_i (\omega\gamma)_i \exp\left(-\frac{E_i}{kT}\right), \quad (9)$$

where  $\mu$  is the reduced mass. We have assumed that the resonance is narrow enough that the partial and total widths can be treated as constants.

When all of our assumptions hold, equation 9 shows that we only need to know the resonance energies and strengths for all resonances that can contribute to know the reaction rate. All three important resonances in  $^{21}\text{Na}(p,\gamma)^{22}\text{Mg}$  are believed to be narrow (see table 1) so that equation 9 can be used for the level of accuracy needed.

### 1.5 Current Knowledge of the $^{21}\text{Na}(p,\gamma)^{22}\text{Mg}$ Reaction Rate, and Spectroscopy of $^{22}\text{Mg}$

At present very few of the parameters needed to determine the  $^{21}\text{Na}(p,\gamma)^{22}\text{Mg}$  reaction rate from equation 9 are known to a reasonable degree of accuracy. Our knowledge of these resonances is summarized in table 1. Figure 2 shows the appropriate excitation regime in  $^{22}\text{Mg}$ , the  $^{21}\text{Na} + p$  threshold, and the mirror nucleus  $^{22}\text{Ne}$ . There are several unresolved questions about the nuclear spectroscopy of  $^{22}\text{Mg}$  that contribute to our lack of knowledge of this reaction rate. A detailed discussion of these nuclear physics issues is given in the appendix, we present a summary here.

There are three important questions about the spectroscopy of  $^{22}\text{Mg}$  that affect the estimated  $^{21}\text{Na}(p,\gamma)^{22}\text{Mg}$  reaction rate. The first of these is the potential presence of unknown resonances. The mirror assignments shown in table 1 imply that such resonances probably do not exist, though there may be some problems with these assignments. The second question is that of the resonance energies. While the uncertainties in the resonance energies of table 1 present experimental difficulties, they are probably not very important for the astrophysical reaction rates. The third question is that of the strengths of the resonances. There are some serious discrepancies in the experimental data that have been used to determine the resonance strengths, and our lack of knowledge of these resonance strengths limits our understanding of the role of the  $^{21}\text{Na}(p,\gamma)^{22}\text{Mg}$  reaction in various astrophysical environments. The availability of a  $^{21}\text{Na}$  beam at ISAC offers an excellent opportunity to measure the strengths of all three resonances, and such a measurement would allow an accurate determination of the  $^{21}\text{Na}(p,\gamma)^{22}\text{Mg}$  reaction rate and a corresponding reduction in our uncertainty in astrophysical  $^{22}\text{Na}$  production. In turn, this would represent a significant advance in our understanding of nucleosynthesis and gamma ray astronomy, among other fields.

$E_r$ (keV)	$E_x$ (MeV)	$J^\pi$	$\tau$ (fs)	$E_x$ (MeV) $^{22}\text{Ne}$	$J^\pi$ $^{22}\text{Ne}$	$\tau$ (fs) $^{22}\text{Ne}$	$\omega_\gamma$ (meV)	Yield $\times 10^{-12}$
212.4(1.9)	5.71	$2^+$	40(15)	6.12	$2^+$	19(8)	2.2	6
336(5)	5.84	$\leq 5$	$\leq 25\text{ns}$	[5.91]	[ $3^-$ ]	[51(23)]	11.3	20
464(25)	5.97	$0^+$	—	6.24	$0^+$	—	2.5	3
770(15)	6.27	$4^+$	$\leq 25\text{ns}$	6.35	$4^+$	—	—	—
1088(33)	6.59	—	—	—	—	—	—	—
1286(19)	6.78	—	—	—	—	—	—	—
1483(80)	6.98	—	—	—	—	—	—	—

Table 1 The resonance parameters for all of the  $^{21}\text{Na}(p,\gamma)^{22}\text{Mg}$  resonances that are accessible with the ISAC beam. Only the first three resonances are important at nova temperatures. The columns marked  $^{22}\text{Ne}$  refer to the appropriate mirror state, and the braces refer to mirror identifications that are tentative; see the appendix for discussion. Numbers in italics are those calculated in [1]; we have used these numbers to make our yield estimates. The yield estimates are for the number of  $^{22}\text{Mg}$  nuclei (or resonant  $\gamma$ -rays) produced per incident  $^{21}\text{Na}$ .

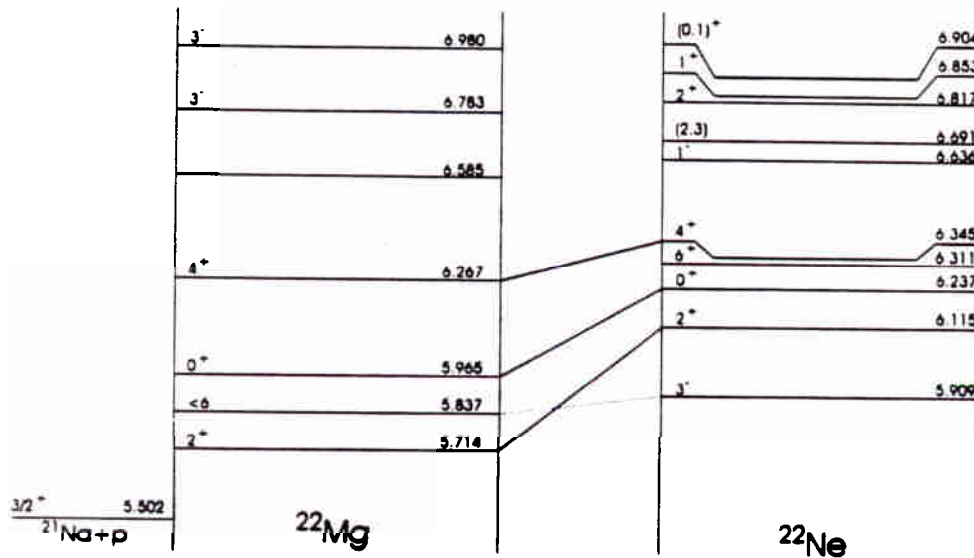


Fig. 2 Level structure of  $^{22}\text{Mg}$  and  $^{22}\text{Ne}$  near the  $^{21}\text{Na}+p$  threshold. All known states in  $^{22}\text{Mg}$  that are accessible with the ISAC beam are shown, along with all known states in the equivalent region of the mirror nucleus  $^{22}\text{Ne}$ . The dashed line represents a tentative mirror identification, no other mirror identifications have been made. While there are at least three missing states in  $^{22}\text{Mg}$  in this region, they are probably too high in excitation energy to affect the astrophysical  $^{21}\text{Na}(p,\gamma)^{22}\text{Mg}$  reaction.

## 2 Experimental Considerations and Plans

### 2.1 Resonance Yields in Thick Targets

In our experiment, the resonance strength will be found by measuring the yield of the  $^{21}\text{Na}(p,\gamma)^{22}\text{Mg}$  reaction for each resonance. Because the resonances of interest are narrow, we will be using a thick target. A detailed discussion of the extraction of resonance strengths from this sort of measurement has been given by Sargood[13]. The energy resolution and energy stability of the ISAC beam energy should be better than 0.2%, and we will use a target that is significantly thicker than this. Then, for our experiment the resonance strength can be directly related to the yield by

$$Y = 2\pi\lambda^2 \omega\gamma \frac{m_p + m_{21}}{m_p} \frac{n}{dE/dx} \int_{E_b - \Delta E}^{E_b} \frac{1}{\sqrt{2\pi}\sigma_b} \exp\left(-\frac{(E - E_R)^2}{2\sigma_b^2}\right) dE, \quad (10)$$

where  $m_p$  and  $m_{21}$  are the masses of the proton and of  $^{21}\text{Na}$ ,  $n$  is the target density in atoms per square centimetre,  $dE/dx$  is the energy loss in keV/(g/cm<sup>2</sup>),  $E_b$  is the beam energy in the centre of mass,  $E_R$  is the resonance energy,  $\Delta E$  is the energy loss of the beam in the target, as observed in the centre of mass frame, and  $\sigma_b$  is the rms deviation of the beam energy. In equation 10 we have neglected straggling of the beam in the target.

To determine  $\omega\gamma$  from our measurements we need to know all of the parameters in equation 10. The most important of these is the energy loss per atom per unit area (i.e.,  $\frac{n}{dE/dx}$ ). Although energy losses for sodium are tabulated (e.g., [14]) and are largely independent of mass, we may have to make some detailed measurements of energy loss in our system. Calibration measurements (see below) will help to clarify this question.

To minimize the sensitivity of our measurements to instability in the beam, and to the energy resolution of the beam it will be important to use a target that is significantly thicker than  $\sigma_b$ , so that the integral in equation 10 is close to one. We plan to use a target thickness of  $2 \times 10^{18}$  atoms cm<sup>-2</sup>. For our planned target length of 10 cm this requires a pressure of about 3 torr at room temperature. We have used the monte carlo code TRIM96 to calculate the energy loss and straggling of the beam in such a target for all three resonances, the results are shown in table 2. The straggling results are consistent with the Bohr estimate for the rms energy straggling which is about 8 keV. While one should not put too much weight on these results, it is clear that this target will be much thicker than the beam energy resolution, the beam straggling, and the line widths of the resonances, so we should not have to worry about these effects broadening the observed resonance, and reducing the observed yield.

Unfortunately, table 2 also shows that, except for the 212 keV resonance, none of the resonance energies are known with sufficient accuracy that we can be confident that we will observe the resonance at any one beam energy. We hope that this situation can be improved through better spectroscopic studies of the levels of  $^{22}\text{Mg}$  before we begin our measurements at ISAC. Should such spectroscopic information not be available when we begin work at ISAC we will either have to work with significantly thicker targets than that discussed above, or we will have to make multiple measurements to determine the resonance energies. Elastic scattering measurements with the ISAC  $^{21}\text{Na}$  beam will probably not help to determine these resonance energies because these resonances are

Resonance Number	cm			lab		
	1	2	3	1	2	3
$E_r$ (keV)	$212.4 \pm 1.9$	$336 \pm 5$	$464 \pm 25$	$4639 \pm 41$	$7340 \pm 110$	$10130 \pm 550$
$E_b$ (keV)	216.2	340	468	4721	7420	10220
$E/A$ (keV/u)				224.8	353	468
$\Delta E$ (keV)	7.6	7.6	7.4	165	165	161
$\sigma_{str}$ (keV)	0.2	0.3	0.6	5	7	14
$\sigma_b$ (keV)	0.4	0.7	0.9	9	15	20
$\Delta\theta$ (°)				0.77	0.62	0.54

Table 2 Experimental parameters for the important  $p(^{21}\text{Na}, \gamma)$  resonances, as seen in the lab and cm frames.  $E_r$  refers to the resonance energy and  $E_b$  to the beam energy we would use to measure the resonance with a target that contains  $2 \times 10^{18}$  atoms  $\text{cm}^{-2}$ .  $\Delta E$  is the energy loss of the beam in the target, and  $\sigma_{str}$  is the straggling in the energy loss (both calculated using TRIM). Straggling is calculated for the beam passing all the way through the target.  $\sigma_b$  is the beam energy resolution (assuming a 0.2% resolution) Finally, the maximum opening angle for the  $^{22}\text{Mg}$  recoils is  $\Delta\theta$ , calculated assuming a ground state gamma ray transition. Gamma ray cascades will reduce the angular spread, though it is still possible to reach the extreme angles

understood to have very small partial particle widths, so these resonances will not be observed in elastic scattering.

One way to allow measurement of resonances whose energy is uncertain is to use a thicker target. The gas target is designed for the  $^{15}\text{O}(\alpha, \gamma)^{19}\text{Ne}$  measurement, and for this reaction the pumps attached to the target may not be able to handle pressures greater than 3 torr. However, the kinematic opening angle of the  $^{19}\text{Ne}$  recoils (due to the gamma decay) is 15.6 mrad, whereas for the 336 keV resonance in  $^{21}\text{Na}(p, \gamma)^{22}\text{Mg}$  it is only 10.8 mrad. This will allow us to use smaller collimators on the downstream side of the target, which should allow us to operate the target at 10 torr without any trouble. This would give a target thickness greater than  $6 \times 10^{18}$  atoms/ $\text{cm}^2$ . At this thickness we could be confident that the 336 keV resonance would be excited in our target, and that we would observe the 464 keV resonance in one of two measurements. On the other hand, the thicker target will certainly lead to greater straggling of both the beam and the recoils, and these effects will probably reduce the beam rejection factor of the electromagnetic separator (EMS). We expect that the EMS will still provide the factor of  $10^{12}$  reduction in beam intensity that will be required to make these measurements, but this effect will, at the very least, increase our observed background.

## 2.2 The DRAGON Facility

The DRAGON facility is being designed to measure capture reactions with ISAC high energy beams. It consists of a gas target, a gamma ray detection array, and a recoil separator that uses electric and magnetic fields to separate the recoiling nuclei from the beam. It is described in more detail elsewhere[15], but we provide a brief description of the facility as it relates to the measurement of the  $^{21}\text{Na}(p, \gamma)^{22}\text{Mg}$  reaction rate



We will use a windowless gas target to measure the  $^{21}\text{Na}(p,\gamma)^{22}\text{Mg}$  reaction rate. We will use a set of four well-collimated surface barrier detectors to observe protons elastically scattered by the beam, two in the vertical plane and two in the horizontal plane. The relative count rates of these sets of detectors will be used to monitor the beam. Background from the decay of the beam will be a concern, but, as will be seen, we should be able to handle it. Although the exact configuration of these detectors is still being studied, a possible configuration would have the detectors at  $20^\circ$ . For the  $^{21}\text{Na}$  beam the Rutherford cross section for scattering to this angle at the 212 keV resonance is about 250 b/Sr. This resonance is understood to be very narrow, so the Rutherford cross section is probably applicable. This will have to be confirmed in preliminary measurements of the elastic cross section. Such measurements could be made in the gas target before the capture measurements begin. The target would be filled with hydrogen, with a known quantity of a heavier gas, for instance argon, added in. A  $^{21}\text{Na}$  beam could then be used to elastically scatter from both gases, and the yields compared. Because the energies that we will be using are so low, the cross section for elastic scattering from the heavy gas can be treated as purely Rutherford, and the absolute yield of  $p(^{21}\text{Na},p)$  elastic scattering can be found.

If the surface barrier detectors view 10% (for instance) of the target they will have a count rate of  $5 \times 10^5$  Hz/Sr. A collimator with a circular aperture of diameter  $1^\circ$  would then have a count rate of 500 Hz. This solid angle represents  $2 \times 10^{-5}$  of  $4\pi$ , and assuming that 1% of the beam will be stopped in the target (we believe that we will be able to do better than this) only 2000 positrons/s will pass through each detector. The observed protons would have energies of 715 keV, which is probably too low to allow the use of a  $\Delta E-E$  telescope, but well above the positron background in a thin detector. Furthermore, the kinematic spread of the protons would be under 10 keV, and the effect of the full energy loss of the beam in the target would be only 15 keV, so significant signal to background improvement could be achieved through good energy resolution. Further background rejection could be achieved by using time of flight techniques; the beam should have a timing resolution of 1 ns, and for a reasonably short flight path a timing resolution of 5 ns with respect to the linac rf should be achievable. Elastically scattered deuterons seen in these detectors would have energies of 1.3 MeV, so the detectors could also be used to monitor the isotopic composition of the target.

Most of the separation of capture products from beam will be done by the EMS of the DRAGON facility. A diagram of the separator showing the tune for the recoiling  $^{22}\text{Mg}$  ions from the 212 keV resonance, along with some of the specifications of the separator is shown in figure 3. The acceptance of the device is large enough to transmit all of the recoils from each of the  $^{21}\text{Na}(p,\gamma)^{22}\text{Mg}$  resonances. Full details of the DRAGON facility can be found in [15]. For the  $^{21}\text{Na}(p,\gamma)^{22}\text{Mg}$  reaction in inverse kinematics, as in all such capture reaction, the momenta of the  $^{21}\text{Na}$  beam and the  $^{22}\text{Mg}$  recoil are essentially identical, but because of the mass difference their energies are quite different ( $\sim 5\%$ ). The EMS has been designed to allow the recoils to pass to the final focus, while the flux of beam particles is reduced by a very large factor. We believe that we can achieve a beam suppression factor better than  $10^{12}$  by the combination of the separator and detection techniques at the final focus. There are four elements in the EMS that separate the recoils from the beam. First, a magnetic dipole is used to select one charge state of the beam and product. Because their momenta are the same, both the beam and product will be focussed at the 'charge selection slit' behind this magnet. We will tune the magnet on the charge state that has the highest abundance. The magnet will allow us to dump all

TRIUMF - ISAC

3rd order  $^{23}\text{Na}(\rho,\gamma)^{23}\text{Mg}$  GIOSP tune

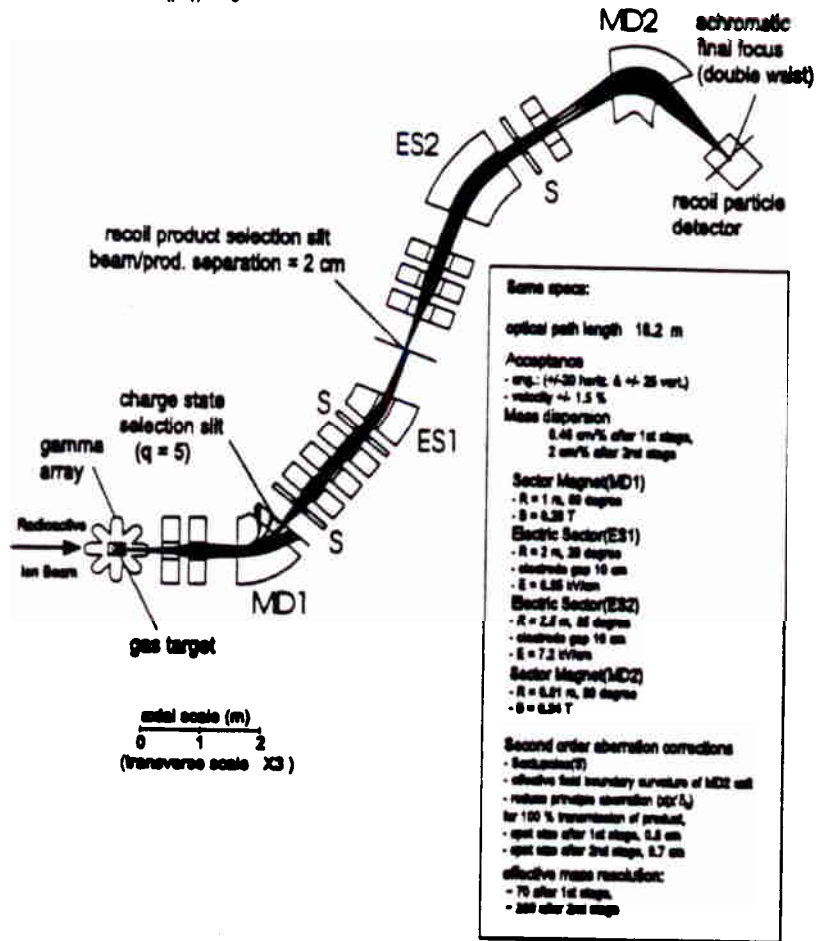


Fig. 3 The DRAGON facility. The tune is shown for five charge states of the recoils and the beam. The recoil/beam separation can be seen at the mid-plane.



of the other charge states of the beam in a controlled manner, to minimize the scattered beam that proceeds down the separator. The next element in the EMS is an electrostatic bender which separates the beam from the product. The beam that has the selected charge state will then be dumped at a well known location at the 'mass selection slit' in the middle of the separator. The recoils will come to a focus of 0.8 cm by 5 cm at this focus, and the beam will be 2.2 cm away from this focus. This separation means that only the tails of the beam can possibly pass through the mass selection slit. Because all of the other charge states of the beam have already been dumped after the magnetic bender, beam scattering on the plates of the electrostatic bender will be minimized. The last two elements of the EMS are another electrostatic bender and another magnetic dipole, both of which have large bend angles. These two elements will be operated as a high resolution mass separator, to perform the final clean up of stray beam particles. The recoils will be brought to a final focus of 6 by 16 mm at the end of the EMS.

We are continuing to investigate the detection techniques to be used at the final focus of the EMS. The fundamental problem that we face is that the recoils that are produced through the interesting resonances have energies from 200-450 keV/u. At such low energies these ions are below the Bragg peak, and so energy losses are not very sensitive to the Z of the ion. In this energy regime all methods of Z-identification that rely on using the Z-dependence of the Bragg curves break down. While we continue to investigate Z-identification techniques, we suspect that we will not be able to make such an identification. This means that we will need excellent background rejection. In order to achieve this rejection we plan to measure as many of the properties of the recoiling nucleus as possible. A possible detector scheme would include the following:

- A thin ( $\sim 5 \mu\text{g cm}^{-2}$ ) carbon foil tilted at about  $30^\circ$  to the incident recoils. This foil would be biased to a few kV, and the secondary electrons induced by passing particles would be accelerated to a nearby micro-channel plate (or more likely, a pair of plates in a chevron configuration). Even for the worst case (the 212 keV resonance) the recoils should lose under 1.5% of their energy in this foil, and suffer an energy straggling of less than 0.2%. A signal from the channel plates themselves would provide a fast (sub-nanosecond) timing signal. The electrons produced in the channel plates would be collected on a resistive anode which would allow determination of the two dimensional position of the event. This position could then be projected onto the foil to determine the location at which the particle hit the carbon foil. This approach should provide position resolution on the mm scale.
- A parallel grid avalanche counter (PGAC) in a chamber full of isobutane. This chamber would be about 50 cm from the carbon foil. The recoiling particles would enter this chamber through a gridded ultra-thin stretched polypropylene foil ( $\sim 40 \mu\text{g cm}^{-2}$ ). Initially, it would pass through (at least) four grids, creating avalanches between pairs of grids. The signals from two of these grids (which would be strung orthogonally to one another) would pass through delay lines to provide x- and y- position information, while either of the other grids can provide a good timing signal. This detector would provide a second position of the detected particle and a time-of-flight relative to the carbon foil. The ions would probably lose somewhat less than 5% of their energy in the PGAC, and about the same amount in the window.
- A segmented ionization chamber. The remainder of the chamber would be separated by wire grids into two or three sections. The charge deposited in each section could

then be determined. The drift time of the electrons would allow a redundant measure of the y-position of the event, and, in principle a  $\Delta E$ -E determination from the relative charge collected in each section. However, as noted above, we will probably not be able to use  $\Delta E$ -E techniques to discriminate between particles of different Z. As a result the relative sizes of the  $\Delta E$  and E signals will probably only be used for redundancy. We do expect to be able to measure the energy with a 2% precision.

This detection scheme would allow us to measure several parameters for the detected heavy ions, thereby increasing our background rejection. The position of the particle at the focal plane of the separator could be measured. Real  $^{22}\text{Mg}$  recoils will come to a focus of 6 by 16 mm. Because we would have measured two positions we will also have measured the angles (vertical and horizontal) that the particle makes with the normal to the focal plane. Again the real recoils should come from the appropriate direction. The two timing measurements allow a time-of-flight to be measured at the the focal plane. Because the positions are known this will allow us to measure the velocity of the particle. Finally, we will also measure  $\Delta E$  and E. The combination of the energy and velocity measurements allows a direct determination of the mass. The mass difference between the beam and the recoil is more than 4.5%; we hope to measure the energies to 2% accuracy and, for the fastest recoils (those from the 464 keV resonance) one ns timing resolution gives a time-of-flight resolution of 2%, measured at the end of the EMS. This should provide a powerful way to discriminate against beam particles. None of these measurements depends upon detection of the gamma ray, which will provide further background suppression.

As mentioned above, we hope to achieve a beam suppression factor of at least  $10^{12}$  using the EMS and the detectors at the end of it. Table 1 shows that with this beam suppression factor we should be able to measure all three of the resonances, although we will be close to our detection limits. While the efficiency for detection of the particle at the focus should be close to 100%, the EMS will only transmit one charge state. For all of the  $^{21}\text{Na}(p,\gamma)^{22}\text{Mg}$  resonances this entails an efficiency of about 35%. Furthermore, the resonance strengths are not well established, and should they prove to be significantly lower than expected we might not be able to measure them with the EMS. In particular, the lowest energy resonance would still be astrophysically significant even if it were much weaker than predicted. Finally, it is worth noting that the lack of Z-discrimination at the final focus makes it essentially impossible, on an event-by-event basis, to discriminate between the two reactions,  $p(^{21}\text{Na},^{22}\text{Mg})\gamma$  and  $p(^{21}\text{Ne},^{22}\text{Na})\gamma$ . Fortunately, there are no known resonances of the second reaction in the energy regions that we will be probing; the only resonance that might be a problem is at 481 keV in the cm, one standard deviation from the 464 keV resonance in  $^{21}\text{Na}(p,\gamma)^{22}\text{Mg}$ . Furthermore, the surface ion source cannot ionize neon, and the natural abundance of  $^{21}\text{Ne}$  is extremely low, so we do not anticipate that there will be a measurable  $^{21}\text{Ne}$  component in the beam. However, we need to confirm that this is the case. This can be done with a higher energy beam so that  $\Delta E$ -E techniques can be used. If we do have problems with the stable beam we should be able to resolve them by closing the slits in the high resolution mass analyzer, at the cost of accepting a lower beam current; the mass difference between  $^{21}\text{Na}$  and  $^{21}\text{Ne}$  is 1 in 6500, within the specifications of the mass separator (1 in 10 000).

The use of the gamma array should resolve the problem of  $^{21}\text{Ne}$  contamination, dramatically improve our beam rejection factor to allow us to measure lower experimental yields, and might allow a more detailed measurement of each resonance. The array will

$E_R$ (keV)	$E_x^1$ (MeV)	$E_x^2$ (MeV)	B.R. (%)
212	5.71	0.0	13±3
		1.25	87±3
336	5.84	1.25	80±15
		3.31	20±15
464 <sup>a</sup>	5.97	5.32	-
		1.25	-

<sup>a</sup>Gamma ray branching ratios for this state are not known. Weisskopf estimates for the two listed transitions are much larger than those for any other transitions. In either case a high energy  $\gamma$ -ray is emitted, either the 4.72 MeV capture  $\gamma$ -ray for the transition to the 1.25 MeV state, or the cascade  $\gamma$ -ray from the 5.32 state, which decays to the ground and first excited states.

Table 3 Gamma ray branching ratios for the  $^{21}\text{Na}(p,\gamma)^{22}\text{Mg}$  resonances. All three resonances will result in the emission of a high ( $> 4$  MeV)  $\gamma$ -ray.

be placed around the target region and will consist of LSO scintillators, which are very fast, bright scintillators. The reaction Q-value for  $p(^{21}\text{Na},^{22}\text{Mg})\gamma$  is 5.5 MeV, and the gamma decays from all three resonances are almost certainly involve the emission of a 4.5-6 MeV gamma ray. On the other hand, the  $p(^{21}\text{Ne},^{22}\text{Na})\gamma$  reaction has a Q-value of 6.7 MeV, and  $^{22}\text{Na}$  has several low lying excited states, so emission of gamma rays with energies greater than 6.5 MeV is likely. The gamma ray energy resolution of the LSO gamma detectors should be about 10%, and should allow us to distinguish between the two reactions. At the cost of efficiency the gamma array will also allow us much better background suppression. We hope to achieve a total gamma ray efficiency of 50%. The simple requirement of a coincidence between a gamma ray of more than 4 MeV and a beam particle at the focus should provide an factor of about 1000 suppression in the background. Furthermore, there is a correlation between the direction of the gamma ray and the direction and momentum of the recoil. For a ground state gamma transition (which is a 13% branch for the 212 keV resonance) there is a simple one to one correspondence, and the angle of gamma emission gives the angle of the recoil directly. This angle will be measured at the focus of the EMS, allowing further background suppression. The measured energy (or time-of-flight) of the recoil could also be compared to the angle of the gamma ray to reduce kinematic broadening. Unfortunately, for all three resonances the dominant transition is to the first excited state (see table 3). Our expected gamma ray energy resolution will allow us to distinguish transitions to the first excited state from transitions to the ground state and the second excited state (3.31 MeV). For the excited state transitions the emission of a 1.25 MeV gamma ray will 'smear out' the angle of the recoil. If we can detect both gamma rays we will still be able to reconstruct the exact angle of the recoil; however, the array of gamma ray detectors will have an efficiency of about 50%, and will be subject to a large flux of annihilation gamma rays that will complicate detection of the 1.25 MeV gamma ray. In the cases where we do not detect this gamma ray, for all of the resonances, it can only change the angle of the recoil by a maximum of 30%, relative to the impulse given by the (4 MeV) capture gamma ray. A comparison of the energy and angle of the recoil with the angle of the capture gamma ray should still allow a considerable reduction in background.

The gamma array may also allow us to make more detailed measurements than would

be available otherwise. The beam energies that we will be using are very low. In fact, the time for the  $^{21}\text{Na}$  beams to cross the 10 cm target range from 10-15 ns. The time resolution of the ISAC beam is about 1 ns, and the LSO scintillators will allow us to measure the arrival time of the gamma ray more accurately than that. Then, in principle, the arrival time of the gamma ray (relative to the rf) will allow us to determine the exact energy at which the capture took place, and therefore to measure the resonance energy. The resonance energy would be given by

$$E_R = E_b - \left( \frac{t_\gamma}{t_{tgt}} \right) \Delta E \quad (11)$$

$$= 216.2 - \frac{t_\gamma}{15 \text{ ns}} 7.6 \text{ keV} \quad (12)$$

in the centre of mass for the 212 keV resonance. In equation 11  $E_R$  and  $E_b$  refer to the resonance and beam energies,  $t_\gamma$  is the arrival time of the gamma ray,  $t_{tgt}$  is the transit time of the beam, and  $\Delta E$  is the energy loss of the beam in the target. A resolving time of one ns would give an energy resolution of 500 eV, which is significantly better than the uncertainty of this resonance energy (1.9 keV). Even for the 464 keV resonance a resolution of 700 eV might be achieved.

Experimentally several factors complicate the use of this time to measure resonance energies. The ISAC beam resolution and stability might be as bad as 0.2%, which would cause a further broadening of the timing by about 0.8 ns, and a further uncertainty of 400 eV in the energy. Straggling of the beam should be more than a factor of two less than this effect (see table 2). The line widths of the  $^{21}\text{Na}(p,\gamma)^{22}\text{Mg}$  resonances are probably in the eV range and should not affect the width of the timing peak. A final complication in this measurement is performing an accurate calibration; the absolute arrival time of the gamma ray is sensitive to a large number of experimental parameters that will need to be understood.

If we can use this technique it would allow us to measure the off-resonance yield at the same time as the resonance yield by simply looking at the arrival time spectrum and comparing the yield in the peak to the yield for the rest of the time that the beam is in the target (i.e., 15 ns of 86 ns between beam bursts for the 212 keV resonance). The centroid of the timing peak would give the energy of the resonance with an accuracy that is potentially as good as 100 eV.

Finally, the angular distribution of the gamma rays as measured by the gamma array will be used to determine the multipolarity of the gamma transition, and thus to confirm the spin-parity assignments of the  $^{21}\text{Na}(p,\gamma)^{22}\text{Mg}$  resonances. In principle the angular distribution of the gamma rays could be deduced from the energy and angular distribution of the recoils. The separator will collect recoils from  $4\pi$  in the centre of mass. The cm angle of the recoil (which is equivalent to the cm angle of the gamma ray for a ground state transition) can be directly related to the energy of the recoil, which is measured at the final focus of the EMS, and to the angle the recoil makes with the focal plane of the separator, which will also be measured. In principle then, the measurements that we will make at the focal plane would allow us to determine the angular distribution of the gamma rays and thus their multipolarity. However, the gamma ray transitions of the  $^{21}\text{Na}(p,\gamma)^{22}\text{Mg}$  resonances are all mostly to the first excited state, so the recoil emits two gamma rays, and its energy and angle are determined by the angles of both gamma rays.

As a result it will be essentially impossible to measure the multipolarity of the gamma ray transition unless we are able to use the gamma array. As noted above, the energy resolution of the gamma detectors should be adequate to differentiate between decays to the ground state, the first excited state at 1.25 MeV, and the second excited state at 3.31 MeV, and to distinguish all three from transitions to the fourth excited state at 4.40 MeV. This resolution will allow us to assign all transitions unambiguously.

While we believe that we will be able to conduct this experiment without the gamma ray array, whether we really are able to do so will depend on the performance of the EMS. On the other hand using the gamma array as part of the DRAGON will essentially ensure that we will have the needed background suppression, and will allow us to obtain much richer information about the  $^{21}\text{Na}(p,\gamma)^{22}\text{Mg}$  resonances.

### 2.3 Experimental Programme

For the purposes of this proposal we will only discuss the measurements that will be necessary to perform the  $^{21}\text{Na}(p,\gamma)^{22}\text{Mg}$  measurement; the DRAGON facility will have to be fully commissioned before we can run, and this will entail many other measurements. Although we have not determined the detailed experimental programme, at the moment we anticipate that we would need to make the following measurements.

First, to ensure that we have all of our equipment set up correctly, and to verify our efficiencies we would propose to measure several known resonances in  $^{21}\text{Ne}(p,\gamma)^{22}\text{Na}$  with a  $^{21}\text{Ne}$  beam. Appropriate resonances are shown in table 4. With a stable beam current of 10 pA the yields from these resonances should be more than adequate for our needs. Because we might have some small  $^{21}\text{Ne}$  contamination in our  $^{21}\text{Na}$  beam (and to determine how much  $^{21}\text{Ne}$  can be tolerated), we would also measure the  $^{21}\text{Ne}(p,\gamma)^{22}\text{Na}$  yield at the energies at which we plan to run  $^{21}\text{Na}$ , i.e., on resonance for each of the three resonances, and above and below each resonance. We emphasize that this experiment will not be possible until an off-line ion source that can produce around 500 nA of  $^{21}\text{Ne}$  is available.

Second, because energy loss is not very sensitive to  $A$ , we would measure resonances in  $^{23}\text{Na}(p,\gamma)^{24}\text{Mg}$  to try to confirm our understanding of the relative energy losses of sodium and magnesium ions in our target. Some appropriate resonances are listed in table 4. These measurements would also allow us to measure charge state distributions for proton capture products; it is possible that the recoil products will not reach equilibrium in our target. A complication to using these data is the fact that the  $Q$ -value for this reaction (11.7 MeV) is much larger than the  $^{21}\text{Na}(p,\gamma)^{22}\text{Mg}$   $Q$ -value (5.5 MeV).

Third, in order to send  $^{22}\text{Mg}$  through the EMS, and also because it is a background for our measurement, we will measure the  $^{21}\text{Na}(d,n)^{22}\text{Mg}$  reaction with the radioactive beam. These measurements will probably have to be made with a deuterated polyethylene target; we may not be able to tolerate deuterium contamination in the gas target. Use of a solid target would reduce our yield by a factor of three, and we would only be able to handle one tenth of the available beam ( $10^{10}$  /s), so we would have only 3% of the yield that would be available if we could use a deuterium gas target. However, deuterium is only .015% of natural hydrogen, so even 3% of the rate that we would get from a gas target represents 200 times the rate of  $^{21}\text{Na}(d,n)$  events that will be observed with a gas



Reaction	E/A (keV/u)	$\omega_\gamma$ (eV)	Yield (/s)
$p(^{21}\text{Ne}, ^{22}\text{Na})\gamma$	269.6(4)	.083(13)	13(2)
$p(^{21}\text{Ne}, ^{22}\text{Na})\gamma$	520.6(15)	.76(15)	60(12)
$p(^{21}\text{Ne}, ^{22}\text{Na})\gamma$	761.9(5)	3.4(9)	180(45)
$p(^{23}\text{Na}, ^{24}\text{Mg})\gamma$	248.9(2)	$5.3(18) \times 10^{-4}$	0.088(30)
$p(^{23}\text{Na}, ^{24}\text{Mg})\gamma$	306.30(6)	.11(2)	14(3)
$p(^{23}\text{Na}, ^{24}\text{Mg})\gamma$	508.0(1)	.091(13)	7.5(11)
$p(^{23}\text{Na}, ^{24}\text{Mg})\gamma$	671.3(4)	.64(11)	40(7)

Table 4 Proposed calibration measurements. The  $p(^{21}\text{Ne}, ^{22}\text{Na})\gamma$  reaction is used because it has the same masses as the  $p(^{21}\text{Na}, ^{22}\text{Mg})\gamma$  reaction, and also because it is a possible background. The  $p(^{23}\text{Na}, ^{24}\text{Mg})\gamma$  involves ions of the same Z as the reaction of interest so it can be used to test energy losses and charge state distributions. The energies are for the heavy ion beams in the lab, and all yields are for a stable beam of 10 pA. Our expected efficiency is about 15%.

target of natural hydrogen. In other words, a few hours of  $^{21}\text{Na}$  beam time at each energy on the solid target will allow us to measure the deuterium induced background in our final measurement. Again, we will need to run at the beam energies for all three resonances (see table 2), and above and below each resonance. Measurements of the mirror to this reaction,  $^{21}\text{Ne}(d,p)^{22}\text{Ne}$  have been performed at 1.5 MeV/amu, and show that the cross sections to the most strongly populated states are less than 10 mb/Sr[16]. The  $d(^{21}\text{Na}, ^{21}\text{Na})n$  cross sections to which we will be sensitive should be much smaller than this because the Coulomb barrier is much higher at our lower energies. Conservatively, we assume a cross section of 20 mb/Sr in the cm. The solid angle of the EMS in the cm is about 0.1 Sr, and deuterium is only 0.015% of natural hydrogen. Thus we expect a yield of  $6 \times 10^{-13}$  for this reaction, which is an order of magnitude lower than the  $(p,\gamma)$  yields listed in table 1. With a deuterated polyethylene target, on the other hand, the same cross section would give a production rate of about 1  $^{22}\text{Mg}$ /s. If we really observe this yield we could use this reaction to produce  $^{22}\text{Mg}$  ions to set up our detectors. At energies around 1.5 MeV/u we could expect to achieve this yield, and we might want to run at such energies during set-up. Because the  $(d,n)$  measurement should have a reasonably high count rate it will also allow us to measure the  $^{21}\text{Ne}$  contamination in the beam, and to study the role that the slits in the ISAC high resolution mass analyzer can play in reducing it. The  $^{22}\text{Na}$  recoils produced by the  $^{21}\text{Ne}$  beam will have energies that differ by 3% from those of the  $^{22}\text{Mg}$  recoils produced 15 by the primary  $^{21}\text{Na}$  beam, so separation of the two components will be straightforward.

Finally, we will perform the  $^{21}\text{Na}(p,\gamma)^{22}\text{Mg}$  measurements themselves. We should have a beam current of  $10^{10}$   $^{21}\text{Na}$  ions/s; yields of  $5 \times 10^7$  /ions/s have already been observed with 1  $\mu\text{A}$  of protons at TISOL. At this beam current the yields for all of the resonances are expected to be greater than several hundred per hour (see below). The efficiency of the EMS should be greater than 30% for the  $^{21}\text{Na}(p,\gamma)^{22}\text{Mg}$  reaction, and we should be able to achieve an efficiency of about 15% for gammas and recoils in coincidence. If we can achieve these rates we should be able to collect enough data on each resonance in a few days. Of course, we will have to run on-resonance and off-resonance for each resonance. If the exact resonance energies of the 336 and 464 keV resonances have not been measured

more accurately by the time this experiment begins we may have to search for them, either by running with a thicker target or by running at as many as ten (for the 464 keV resonance) different energies.

We will also undertake complementary measurements of the elastic scattering of  $^{21}\text{Na}$  by protons. As noted above, elastic scattering measurements will be necessary to normalize the yields measures in the capture reactions. In addition, measurement of elastic scattering through the higher lying resonances in  $^{21}\text{Na}+p$  could provide spectroscopic information about the corresponding states in  $^{22}\text{Mg}$ . This could then allow us to make mirror identifications for these states, and to learn more about the Thomas-Ehrmann shifts in  $A=22$  nuclei. With a better understanding of these shifts, we could have greater confidence that there are no unknown resonances in  $^{21}\text{Na}(p,\gamma)^{22}\text{Mg}$  that could play an important role in the astrophysical reaction rate. Precise measurement of the resonance energies of these states coupled with precision measurements of the excitation energies of the same states could also improve the uncertainty in the  $^{21}\text{Na}(p,\gamma)^{22}\text{Mg}$  Q-value, which is currently 1.5 keV. We would plan to make these measurements in the general purpose scattering chamber in the ISAC high energy hall, using a stretched polyethylene target. This target would limit beam currents to about  $10^9$  ions/s; higher current would cause unacceptable target degradation. Furthermore, to monitor the target stoichiometry we would have to measure scattering with stable beam at regular intervals.

Everything that we need to complete this experimental programme should be available quite early in the life of the ISAC facility. Even if the gamma array is not available when ISAC becomes operational, we should still be able to measure the important  $^{21}\text{Na}(p,\gamma)^{22}\text{Mg}$  resonances, or at the very worst put meaningful upper limits on them. Because of this, because our expected count rates are quite high (see below), and because of the importance of this reaction rate in various fields of astrophysics, this experiment is well suited to be the first nuclear astrophysics measurement made at ISAC.

### 3 Beam Time required

The expected count rate for the 212 keV resonance can be estimated as follows: The expected yield for the calculation of [1] is  $6 \times 10^{-12}$  (see table 1). With a beam of  $10^{10}$  ions/s we expect to have 0.06  $^{22}\text{Mg}$  recoils produced per second, or 200 /hr. The total detection efficiency of the DRAGON (including the gamma detectors) is 15%, or 30 counts/hour. In 48 hours we should have 1400 counts, which would allow us to be sensitive to resonance strengths about one order of magnitude smaller than the estimate of [1]. Times for all of the work are shown in table 5. We have allowed for twice the number of counts for the 212 keV resonance because it is the most important astrophysically. To some extent these estimates depend on our (optimistic) estimates of the time needed to change beam energies and to switch between stable and radioactive beams.

Note also that these estimates are exclusive of dedicated stable beam time for the commissioning of the DRAGON, and of stable beam time required in preparation for radioactive beam time, and for the calibrations discussed above.



Measurement	Count Rate (/hr)	Time Required
Runs at 233, 225, and 217 keV/u (212 keV resonance)	30	12 shifts
Runs at 361, 353, and 345 keV/u (336 keV resonance)	100	2 shifts
Runs at 520, 495, and 471 keV/u (464 keV resonance)	15	12 shifts
Measurement of higher resonances and (d,n)		10 shifts
Elastic Scattering		12 shifts
Contingency		24 shifts
		54 shifts

Table 5 Estimated beam time requirements

#### 4 Electronics and Acquisition

We are assuming that the infrastructure for conducting our experiment will be in place when we begin our experimental programme. We will need the electronics for the focal plane detectors and the gamma array[15], and would plan to use the ISAC data acquisition system. While we might require additional computing power for our analysis we would expect to obtain funding for this from NSERC.

#### 5 Appendix: Spectroscopy of $^{22}\text{Mg}$ and the $^{21}\text{Na}(p,\gamma)^{22}\text{Mg}$ Reaction Rate

As discussed in section 1.5, there are three important factors needed to determine the reaction rate for reactions that proceed through narrow isolated resonances. We will consider the role that each of these plays in the uncertainty in the  $^{21}\text{Na}(p,\gamma)^{22}\text{Mg}$  reaction rate.

##### 5.1 Completeness of Level Scheme

For astrophysics the most important question that needs to be addressed by spectroscopy of  $^{22}\text{Mg}$  is the question of whether there is an unknown resonance in the  $^{21}\text{Na} + p$  system that affects the  $^{21}\text{Na}(p,\gamma)^{22}\text{Mg}$  reaction rate. Of particular concern is the possible existence of an unknown resonance with an energy less than about 500 keV, which would correspond to an excitation energy in  $^{22}\text{Mg}$  between 5.5 and 6.0 MeV. A comparison between  $^{22}\text{Mg}$  and its well studied mirror nucleus,  $^{22}\text{Ne}$  shows that the only known state in  $^{22}\text{Ne}$  with an excitation energy less than 6.6 MeV that has not been assigned a mirror state in  $^{22}\text{Mg}$  is a  $J^\pi = 6^+$  state at 6.31 MeV[17] (see figure 2). The mirror to this state would be a  $f$ -wave resonance at around 800 keV in  $^{21}\text{Na}+p$ , and therefore would be very unlikely to contribute to the  $^{21}\text{Na}(p,\gamma)^{22}\text{Mg}$  reaction rate. At excitation energies above 6.6 MeV there is one 'missing' state at 6.6 MeV, and several missing states around 6.8 MeV. These states would correspond to resonance energies greater than 1 MeV, and at

temperatures appropriate for explosive hydrogen burning they are probably not important. These mirror assignments suggest that it is unlikely that there is an unknown state in  $^{22}\text{Mg}$  that could act as a resonance in the  $^{21}\text{Na}(p,\gamma)^{22}\text{Mg}$  reaction at astrophysical energies. However, one should also note that five of the mirror assignments of states below and near the  $^{21}\text{Na}+p$  threshold are tentative, so it is possible that such a resonance does exist. Further spectroscopy of  $^{22}\text{Mg}$  could resolve this question; this work would be more readily accomplished with stable beams than with the  $^{21}\text{Na}$  beam at ISAC. In the likely event that the level structure of  $^{22}\text{Mg}$  near the  $^{21}\text{Na}+p$  threshold is complete we need only concern ourselves with the three known states that have excitation energies of 5.71, 5.84, and 5.97 MeV.

## 5.2 Resonance Energies

As table 1 show, the energies of the three astrophysically important resonances in  $^{21}\text{Na}(p,\gamma)^{22}\text{Mg}$  are reasonably well known. The uncertainty of 1.9 keV in the energy of the lowest energy resonance leads to an uncertainty in the reaction rate of about 50% at a temperature of  $T_9 = 0.05$ , at which temperature the  $^{21}\text{Na}(p,\gamma)^{22}\text{Mg}$  reaction rate is almost certainly negligible. This uncertainty decreases at higher temperatures. The 5 keV uncertainty on the second resonance leads to a 30% uncertainty in the rate through this resonance at  $T_9 = 0.2$ , and below this energy this resonance is probably not important. Finally, the 25 keV uncertainty in the energy of the 470 keV resonance leads to an uncertainty of 70% in the reaction rate through this resonance at  $T_9 = 0.4$  where it begins to be important, and this uncertainty is probably not excessive either, especially as it is argued in [1] that the first resonance dominates the rate. However, the large uncertainty in the energy of this resonance will be a problem experimentally.

## 5.3 Resonance Strengths

The resonance strength is not known for any of the  $^{21}\text{Na}(p,\gamma)^{22}\text{Mg}$  resonances. The resonance strength is defined as

$$(\omega\gamma)_i = \frac{2J_i + 1}{(2J_p + 1)(2J_{21} + 1)} \frac{\Gamma_p^i \Gamma_\gamma^i}{\Gamma_{TOT}^i}; \quad (13)$$

to determine the resonance strengths from spectroscopic information about  $^{22}\text{Mg}$  we must know all of these parameters. We will discuss each of the three resonances in turn:

**212 keV** This resonance has been assigned  $J^\pi = 2^+$  based on angular distributions of transfer reactions[17]. Furthermore, its lifetime has been measured to be  $40 \pm 15$  fs[18], which corresponds to a total width of  $16 \pm 6$  meV. Note that the lifetime result is consistent with zero at the  $3\sigma$  level. The partial widths are unknown.

The fact that the measured width of this state is so narrow is a little puzzling. If the state has  $J^\pi = 2^+$  it can absorb *s*-wave protons. One would expect an *s*-wave resonance to have a large proton width, larger, in fact, than the measured total width. To explain this discrepancy Wiescher et al.[11] assume a very small reduced proton width (i.e., they assume that the overlap of the  $^{21}\text{Na}+p$  wave function with the

wave function of the resonant state is very small). However, as noted by Wiescher and Langanke[1], a comparison with the mirror of this state in  $^{22}\text{Ne}$  shows that it has a large (410 keV) Thomas-Ehrmann shift, which implies that the state has a large reduced proton width. The combination of an appropriately chosen reduced proton width and an  $s$ -wave resonance leads to a proton partial width that is more than an order of magnitude larger than the measured width[1] (although not inconsistent with it at the  $3\sigma$  level). Wiescher and Langanke resolved this discrepancy by assuming that this is a  $d$ -wave resonance, and that the partial width for  $s$ -wave proton emission is small enough that it can be neglected. Assuming that this state has this unusual structure they find a reduced proton width of about 0.5, and  $\Gamma_p \approx 5$  meV. From this result they deduce that  $\omega\gamma = 2.2$  meV. Unfortunately, even this explanation of the experimental data has problems; studies of the  $^{21}\text{Ne}(d,p)^{22}\text{Ne}$  reaction have found that none of the states between 5.6 MeV and 6.6 MeV in  $^{22}\text{Ne}$  are populated by stripping[19]. This implies that all of these states have very small reduced neutron widths, and therefore that their mirror states in  $^{22}\text{Mg}$  have very small reduced proton widths. (i.e., much smaller than the 0.5 used in [1].) Two possible explanations for the discrepancy between the large Thomas-Ehrmann shift and the presumably small proton width of this state is that this state has a large overlap with the first excited state of  $^{21}\text{Na}$ , or that the mirror identification is incorrect. The first excited state of  $^{21}\text{Na}$  is a  $5/2^+$  state at 332 keV, as a result the 5.71 MeV state in  $^{22}\text{Mg}$  is bound with respect to decay to this state by 120 keV. However, it is still possible that the state has a large reduced width with regards to decay to this state, and that this width leads to the large observed Thomas-Ehrmann shift. Alternately, if the mirror identification of [17] for the 5.71 MeV state is incorrect, the Thomas-Ehrmann shift might be much smaller than it is currently believed to be. There are no  $2^+$  states available in  $^{22}\text{Ne}$  as alternate mirror states to this state with the appropriate excitation energies, so for the mirror identification to be in error there must be an unknown state in the well-studied nucleus  $^{22}\text{Ne}$ . The discrepancy between the Thomas-Ehrmann shift of this level on the one hand, and its total width and the reduced width of its mirror state on the other has no obvious solution. This problem means that the resonance strength used by [1] cannot be used with any great confidence, however, we have adopted their strength in our yield estimates. **because other estimates are probably even worse.**

**336 keV** The  $J^\pi$  assignment for this state is not as certain as that of the other two resonances that we will consider; in fact the only measurement that has constrained the spin of this resonance is that of Grawe et al.[18] who assign it to have  $J \leq 5$ . Fortunately, this is the only state in the region of excitation in  $^{22}\text{Mg}$  that has not been assigned a mirror state in  $^{22}\text{Ne}$ [17]. Only the 5.91 MeV state in  $^{22}\text{Ne}$  has not been assigned a mirror state in  $^{22}\text{Mg}$ , so it is natural to assign these two states to be mirror states. Our estimates of the strength of this resonance rely on this identification.

Once this mirror identification is made we can assume that  $J^\pi$  for this resonance is  $3^-$ , which implies that it is a  $p$ -wave resonance. From the Thomas-Ehrmann shift, Wiescher and Langanke[1] calculate a partial proton width of 1.1 eV. The lifetime of the (bound) mirror state in  $^{22}\text{Ne}$  is  $51 \pm 23$  fs, and if this resonance has the same partial gamma width then  $\Gamma_\gamma = 13 \pm 6$  meV. From this result Wiescher and Langanke deduce  $\omega\gamma = 11.3$  meV. Because the partial proton width is much bigger

than the partial gamma width, by equation 13 the calculated resonance strength is not sensitive to uncertainties in the partial proton width. However, note that the lifetime of the mirror state is consistent with zero (certainly at the  $3\sigma$  level). This implies that the resonance strength is consistent with, for example, 1 eV, though such a large strength is *a priori* unlikely. (It may be relevant to note that the Weisskopf estimate for the partial gamma width of the state in  $^{22}\text{Mg}$  is 50 eV.) So the strength of this resonance is not very well known from the spectroscopy of  $^{22}\text{Mg}$ . It also needs to be measured.

**464 keV** There is strong experimental evidence for the spin-parity ( $0^+$ ) and mirror assignments for this resonance. Unfortunately, the lifetime of the mirror state is not known experimentally. From the Thomas-Ehrmann shift Wiescher and Langanke deduce a partial proton width of 5 eV, and from gamma ray statistics assume a partial gamma ray width of 20 meV. This gives  $\omega\gamma = 2.5$  meV. However, the reduced proton width that they assume (0.3) is inconsistent with (d,p) measurements of the mirror state, which was not populated[19]. For this state  $\Gamma_\gamma \ll \Gamma_p$ , so  $\omega\gamma$  is not very sensitive to the partial proton width, and thus to the reduced width (see equation 13). But, when one considers this discrepancy and the fact that gamma ray statistics were used to estimate the partial gamma width of this resonance, it is clear that the importance of this resonance to the  $^{21}\text{Na}(p,\gamma)^{22}\text{Mg}$  rate is not known. It will probably only play a role at relatively high nova temperatures, but until the resonance strength is known we cannot be certain.

From this discussion it is clear that a measurement of the resonance strengths of these three resonances will dramatically improve our understanding of the  $^{21}\text{Na}(p,\gamma)^{22}\text{Mg}$  reaction rate. This, of course, is exactly what we propose to do.

## References

1. M. Wiescher & K.-H. Langanke, *Z. Phys. A*, **325**, 309 (1986)
2. D.C. Black, *Geochim. Cosmochim. Acta*, **36**, 377 (1972)
3. M. Arnould & H. Neorgaard, *A.&A.*, **64**, 195 (1978)
4. U. Ott, *Nature*, **364**, 25 (1993)
5. E. Zinner, in *Nuclei in the Cosmos III, AIP proceedings 327*, eds. M. Busso, R. Gallino, C.M. Raitieri, AIP press, Washington D.C. (1995) p. 567
6. M. Politano, S. Starrfield, J.W. Truran, A. Weiss, and W.M. Sparks, *Ap.J.*, **448**, 807 (1995)
7. M.F. Bode & A. Evans *Classical Novae*, John Wiley & Sons Ltd., Chichester, U.K., (1989)
8. A.F. Iyudin, K. Bennett, H. Bloemen, R. Diehl, W. Hermsen, G.G. Lichti, D. Morris J. Ryan, V. Schönfelder, H. Steinle, A. Strong, M. Varendorff and C. Winkler, *A.&A.*, **300**, 422 (1995)
9. M. Leising *Bull. Am. Phys. Soc.*, **42**, No. 2, J1, 1, p. 1061 (1997)
10. A. Coc, R. Mochkovitch, Y. Oberto, J.-P. Thibaud and E. Vangioni-Flam *A.&A.*, **299**, 479 (1995)
11. M. Wiescher, J. Görres, F.K. Thielemann and H. Ritter *A.&A.*, **160**, 56 (1986)
12. C.E. Rolfs & W.S. Rodney, *Cauldrons in the Cosmos*, University of Chicago Press, Chicago (1988)
13. D.G. Sargood, *Phys. Rep.*, **93**, 61 (1982)
14. J.F. Ziegler, J.P. Biersack & U. Littmark, *The Stopping and Range of Ions in Solids*, Pergamon Press, New York (1985)
15. submission to TRIUMF EEC, 1997
16. B. Chambon et al. *Nucl. Phys.*, **A136**, 311 (1969)
17. P.M. Endt *Nucl. Phys.*, **A521**, 1 (1990)
18. H. Grawe, K. Holzer, K. Kändler and A.A. Pilt *Nucl. Phys.*, **A237**, 18 (1975)
19. P. Neogy, R. Middleton and W. Scholz *Phys. Rev. C*, **6**, 885 (1972)

